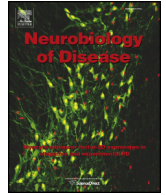




Contents lists available at ScienceDirect

Neurobiology of Disease

journal homepage: www.elsevier.com/locate/ynbdi

Cisplatin induces mitochondrial deficits in *Drosophila* larval segmental nerve

Jewel L. Podratz^a, Han Lee^b, Patrizia Knorr^a, Stephanie Koehler^a, Steven Forsythe^a, Kelsey Lambrecht^a, Suzette Arias^a, Kiley Schmidt^a, Gabrielle Steinhoff^a, Georgiy Yudintsev^b, Amy Yang^a, Eugenia Trushina^{a,b,1}, Anthony Windebank^{a,*}

^a Department of Neurology, Mayo Clinic, Rochester, MN, USA

^b Department of Molecular Pharmacology and Experimental Therapeutics, Mayo Clinic, Rochester, MN, USA

ARTICLE INFO

Article history:

Received 15 February 2016

Revised 4 October 2016

Accepted 16 October 2016

Available online xxxx

Keywords:

Mitochondria

Cisplatin

Motor neuron

Drosophila

Axonal trafficking

Membrane potential

Apoptosis

ABSTRACT

Cisplatin is an effective chemotherapy drug that induces peripheral neuropathy in cancer patients. In rodent dorsal root ganglion neurons, cisplatin binds nuclear and mitochondrial DNA (mtDNA) inducing DNA damage and apoptosis. Platinum-mtDNA adducts inhibit mtDNA replication and transcription leading to mitochondrial degradation. Cisplatin also induces climbing deficiencies associated with neuronal apoptosis in adult *Drosophila melanogaster*. Here we used *Drosophila* larvae that express green fluorescent protein in the mitochondria of motor neurons to observe the effects of cisplatin on mitochondrial dynamics and function. Larvae treated with 10 µg/ml cisplatin had normal survival with deficiencies in righting and heat sensing behavior. Behavior was abrogated by the pan caspase inhibitor, p35. However, active caspase 3 was not detected by immunostaining. There was a 27% decrease in mitochondrial membrane potential and a 42% increase in reactive oxygen species (ROS) in mitochondria along the axon. Examination of mitochondrial axonal trafficking showed no changes in velocity, flux or mitochondrial length. However, cisplatin treatment resulted in a greater number of stationary organelles caused by extended pausing during axonal motility. These results demonstrate that cisplatin induces behavior deficiencies in *Drosophila* larvae, decreased mitochondrial activity, increased ROS production and mitochondrial pausing without killing the larvae. Thus, we identified particular aspects of mitochondrial dynamics and function that are affected in cisplatin-induced peripheral neuropathy and may represent key therapeutic targets.

© 2016 Elsevier Inc. All rights reserved.

1. Introduction

Cisplatin-induced peripheral neuropathy is a dose-limiting side effect occurring in 30–40% of cancer patients (Johnson et al., 2015; Windebank and Grisold, 2008). Symptoms are mainly sensory including tingling, numbness, paresthesia and pain (Cavaletti and Marmiroli, 2010; O'Reilly et al., 2014). Some patients experience a worsening of the sensory symptoms for 2–6 months after completion of their treatment, which is a phenomenon known as “coasting” (Miltenburg and Boogerd, 2014; Reinstein et al., 1980). Long-term neuropathy lowers quality of life for many cancer survivors and currently there are no preventive therapies for cisplatin-induced peripheral neuropathy. Chronic neurotoxicity is also caused by the other commonly used platinum compounds, carboplatin and oxaliplatin. Understanding the underlying mechanisms of chemotherapy-induced peripheral neuropathy (CIPN)

is critical for the development of effective therapeutic approaches (Albers et al., 2011).

Cisplatin neurotoxicity is attributed to the formation of platinum-DNA (Pt-DNA) adducts leading to cellular stress and apoptosis (Eastman, 1987; McDonald et al., 2005). Cisplatin binds both nuclear DNA (nDNA) and mitochondrial DNA (mtDNA) inducing DNA damage and apoptosis in rat dorsal root ganglion (DRG) neurons, in vitro (McDonald et al., 2005; McDonald and Windebank, 2002; Podratz et al., 2011a; Ta et al., 2006; Ta et al., 2009). Cisplatin binds nDNA leading to upregulation of p53, cell cycle re-entry and translocation of BCL2-associated X (bax) protein to the mitochondria (Fischer et al., 2001; Gill and Windebank, 1998; McDonald and Windebank, 2002). Cisplatin also binds mtDNA inhibiting replication and transcription leading to mitochondrial degradation (Podratz et al., 2011a). Accumulation of Pt-DNA adducts is higher in DRG neurons although the rate of repair is similar to other cell types (McDonald et al., 2005). Pt-DNA adducts are removed by nucleotide excision repair in the nucleus. However, this mechanism does not exist in mitochondria (Croteau et al., 1999; Larsen et al., 2005). Pt-mtDNA adducts may play an important role in the mechanism of cisplatin-induced neurotoxicity.

* Corresponding author at: 200 First Street SW, Rochester, MN 55905, USA.

E-mail address: windebank.anthony@mayo.edu (A. Windebank).

¹ Additional senior author.

Available online on ScienceDirect (www.sciencedirect.com).

Differentiating the effects of Pt-nDNA and Pt-mtDNA adducts on DRG neurons in culture is challenging. nDNA damage can have profound effects on mitochondria through p53 and bax translocation and mitochondrial stress can independently initiate apoptosis (Savitskaya and Onishchenko, 2015). Our previous studies showed that cisplatin induced a neuron specific climbing deficiency in adult *Drosophila melanogaster* (Podratz et al., 2011b). Adult flies fed 50 µg/ml cisplatin for three days formed DNA adducts at the same rate as rat DRG neurons in vitro and induced climbing deficiencies associated with neuronal apoptosis. Imaging of motor neuron mitochondria dynamics and function can be done in live *Drosophila* larvae (Shidara and Hollenbeck, 2010). This allows for examination of mitochondrial dynamics and neuronal apoptosis in relation to larval behavior and survival. Our studies utilized a genetically modified fly with a motor neuron driver, *P[GawB]D42*, (Yeh et al., 1995) and a GFP responder targeted to the mitochondria *P[w⁺mC = UAS-mitoGFPAP3*] (Pilling et al., 2006) on the third chromosome. These flies expressed GFP specifically in mitochondria of motor neurons and were used to observe the direct effects of cisplatin on mitochondria in the intact nervous system of live larvae. Motor neuron segmental nerves of the *Drosophila* larvae represent an ideal model system to study mitochondrial function and axonal transport in vivo.

2. Materials and methods

2.1. Flies and reagents

Cisplatin was obtained from APP (Lake Zurich, IL) as an aqueous stock solution of 1 mg/ml in saline. The fly strain (*w*; *+/+*; *D42-GAL4 P{UAS-mitoGFP} e/TM6B, Tb Hu e*) was a gift from Dr. P. Hollenbeck (Purdue University, IN). *w*[*]; *P[w⁺mC = UAS-mitoGFPAP3]* *GawB]D42* flies were purchased from Bloomington *Drosophila* Stock Center (Bloomington, IN). *UAS-p35* flies were obtained from Bruce Hay's Laboratory (California Institute of Technology). Instant fly food was purchased from Carolina Biologicals (Burlington, NC).

2.2. *Drosophila* larval drug treatment

Drosophila larvae were age synchronized and treated with or without cisplatin for 3 days (Fig. 1A). On day 1, 150–200 adult flies (*w*; *+/+*; *D42-GAL4 P{UAS-mitoGFP} e/TM6B, Tb Hu e*) were added to an embryo collection chambers containing grape agar plates and

yeast paste. Chambers were placed into a 25 °C environmental chamber for 18–24 h. On day 2, adults were removed and the embryos were placed back into a 25 °C environmental chamber for another 24 h. On day 3, first instar larvae were removed from the grape agar plates and placed into the chamber containing instant food overnight at 25 °C. On day 4, larvae were collected and treated with cisplatin for all experiments. Second instar larvae were collected using a sieve and twenty larvae per each experimental group were placed into chambers with instant food rehydrated with and without cisplatin.

2.3. Larval dissection

Drosophila larvae were dissected to expose the segmental nerves for live imaging (Fig. 1B). Wandering third instar larvae treated with and without cisplatin were removed from the wells and washed in water to remove food. The larva was transferred to a Sylgard plate and pinned ventral side down. An insect pin was first placed at the posterior end of the larva between tracheal tubes followed by a second pin at the anterior end near the “beak”. Using fine scissors, a small incision at the posterior end of the larva was made following with a longitudinal cut from the posterior to anterior. 400 µl of HL6 buffer (see Supplemental data) was added on top of the larva. Using forceps, tracheal tubes and fat bodies were removed starting at the posterior end. The buffer was removed and 400 µl of fresh HL6 buffer was added to the larva to remove debris. Small lateral incisions were made on the posterior and anterior ends perpendicular to the longitudinal cut to allow the body wall to open and the larvae to lie flat for imaging. The larva was mounted onto a special chamber slide with HL6 buffer containing 10 mM glutamate to desensitize glutamate receptors and decrease muscular movements.

2.4. Larval survival assay

Drosophila larvae were drug treated as described above and observed for survival to the pupae and adult developmental stages. Twenty larvae per condition were placed into vials containing 0, 1, 5, 10, 25, and 50 µg/ml cisplatin in instant food. All treatments were conducted in duplicates. Larvae were observed for another seven to nine days. Pupae were counted on day 10 of the assay, and the number of adults that hatched from those pupae was counted on day 12–14. Survival rates were determined from 100 to 180 larvae as the number of pupae or adults verses the total number of larvae added to the vial.

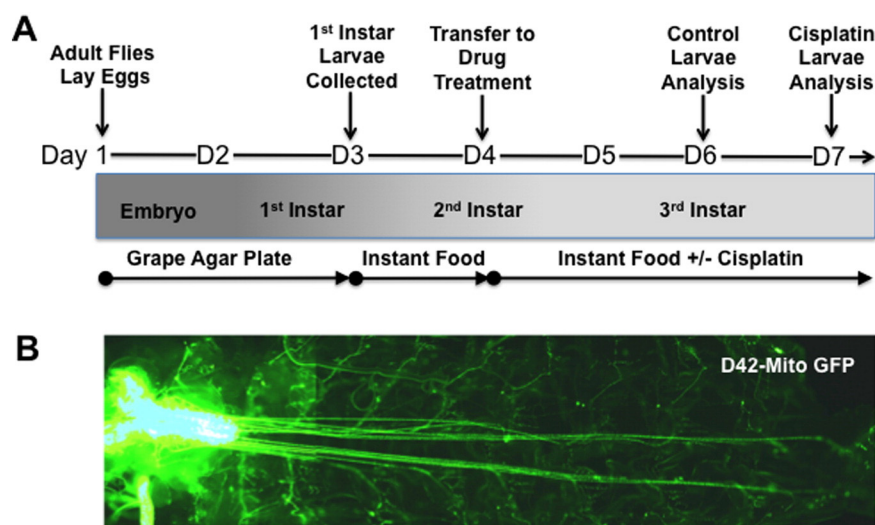


Fig. 1. Experimental model. (A) Schematic diagram of synchronization of larvae developmental stages and drug treatment. (B) Image of dissected larva with exposed motor neurons and segmental nerves. Larvae image was acquired using a Zeiss AxioScope (Carl Zeiss, Thornwood, NY) with a 40× lens.

2.5. Larval behavior assays

Larvae were treated with and without cisplatin and behavior assays were conducted at the wandering third instar larva developmental stage. Untreated larvae were assessed on day 6 and cisplatin treated larvae were tested on day 7 due to a cisplatin-induced 24 hour delay in development. Behavior assays were conducted on both D42-MitoGFP and D42-p35 larvae. Using the GAL4-UAS system, we expressed p35 in *Drosophila* larvae using a D42 motor neuron specific driver. These flies were used to determine if any behavior changes we observed involved caspase activation.

2.5.1. Righting assay

Following drug treatment, the larvae were washed with water and placed in a room temperature grape agar plate to assess righting behavior. When larvae were actively moving in a straight path, they were flipped onto their dorsal side. Using a stopwatch, the larva was timed for how long it took to flip back onto its ventral side and resume crawling. The larvae were behaviorally conditioned to righting themselves three times. A minimum of 10 s was used between flips and timed flips were performed 5 times for each larva. Righting was determined in 14–60 D42-MitoGFP larvae and 14–15 D42-p35 larvae.

2.5.2. Crawling assay

To assess crawling behavior, larvae were washed and placed onto a glass petri dish containing 2% agarose. The petri dish was then placed on grid paper with 0.635 cm squares and larvae were left for 30–60 s to reorient themselves. Once the larva began to crawl, the number of squares the larvae entered in 1 min was counted. This was repeated 5 times for each larva. Crawling was observed in 30–35 D42-MitoGFP larvae and 14–15 D42-p35 larvae.

2.5.3. Heat sensing assay

Larvae were assessed for their ability to sense heat. A block heater was heated to a stable 70 °C and the temperature checked before the beginning of each experiment. A larva was placed into 80 µl of deionized water inside an open plastic petri dish. The dish containing the larva was placed on the hot plate and a timer started. The larva was observed using a Zeiss STEMI SR Stereomicroscope (Carl Zeiss, Thornwood, NY). When head thrash behavior was observed, the timer was stopped. Each larva was assessed only one time. Heat sensing was observed in 20–27 D42-MitoGFP and 14–15 D42-UAS-p35 larvae.

2.6. Active caspase 3 immunostaining

Larvae were treated with 0, 10 and 25 µg/ml cisplatin and dissected as previously described. Larvae were fixed in 4% paraformaldehyde for 20 min, treated with 0.1% Triton X-100 for 30 min and blocked using 0.1% Triton X-100 with 5% inactivated normal goat serum (NGS) for another 30 min at RT. Larvae were incubated with 1:1000 rabbit anti-caspase 3 antibody (Life Technologies, Grand Island, NY) in 5% NGS overnight at 4 °C. For the negative control, no primary antibody was added. The tissue was re-blocked with 0.1% Triton X-100 and 5% NGS and incubated with 1:400 anti-rabbit-Cy3 antibody (Jackson Labs.) in 5% NGS overnight at 4 °C. Tissue was prepared for fluorescence microscopy using Vectashield mounting medium (Vector Labs, Burlingame, CA). Images were acquired using a LSM 780 Axio Observer microscope with a 40× lens (C-apochromat/1.20 W) for fluorescence detection (excitation/emission: 490/533 (green) and 566/685 (red)) (Carl Zeiss, Thornwood, NY).

2.7. Mitochondria membrane potential and reactive oxygen species production

Mitochondria from cisplatin treated larvae were observed for membrane potential (MMP) using tetramethylrhodamine methyl ester

(TMRM) and Reactive Oxygen Species (ROS) using MitoSox. Larvae were treated with 0, 10 or 25 µg/ml cisplatin, tested for righting behavior and dissected as described above. Larvae were exposed to 400 µl of 1 µM TMRM in HL6 buffer in the dark for 20 min at room temperature and TMRM was removed. Larvae were mounted in HL6 buffer as described above and distal nerve segments were examined using an Olympus Multiphoton Laser Scanning microscope with a 60× lens (UPLSAPO/1.2 W) for fluorescence detection (excitation/emission: 488/520 (green) and 543/583 (red)) (Olympus, Waltham, MA). The number of green (GFP) mitochondria and the number of red (TMRM) organelles were counted in 34–79 distal nerve segments from 17 to 38 larvae and results were expressed as a percent of mitochondria that expressed both red and green fluorescence. To determine mitochondrial density, distal nerve segments were quantitated for the percent of green (GFP) area using Image J software.

To determine whether cisplatin induced an increase in ROS production, larvae were treated with 0 and 10 µg/ml cisplatin, dissected as described above and exposed to 5 nM MitoSox for 20 min. Distal nerve segments were examined by confocal microscopy (Olympus Multiphoton Laser Scanning microscope (FV1000MPE)) with a 60× lens (LUMFLN/1.1 W) for fluorescence detection (excitation/emission: 488/520 (green) and 543/583 (red)). Levels of green (GFP, mitochondria) and red (MitoSox, ROS) fluorescence mean intensity were measured by outlining 26–41 distal nerve segments and measuring the mean intensity of fluorescence from 7 to 16 larvae imaged under the same conditions. Fluorescence intensity was presented as a ratio of red to green fluorescence.

2.8. Axonal trafficking assay

Larvae were treated with 0, 10 and 25 µg/ml cisplatin, dissected and mounted onto special chamber slides as previously described. Imaging of live larvae was performed using an Olympus Multiphoton Laser Scanning microscope (FV1000MPE) using a 60× (UPLSAPO/1.2 W) for fluorescence detection (excitation/emission: 488/520 (green)). Larvae distal nerve segments were imaged every second for 10 min and converted to an .avi movie format for trafficking measurements. A total of 1–2 nerve segments per larva and 16–17 larvae were measured per condition. Experiments were conducted at room temperature. For best visualization of moving mitochondria, an area of the distal motor axon was photo bleached for 10 s followed by imaging of unbleached mitochondria entering the bleached area. Analysis of axonal trafficking was conducted using Image J software (NIH, Bethesda, ME). The distance the mitochondria moved was measured from frame to frame and velocity was calculated as the average distance traveled per second. The coordinates of a stationary mitochondrion were used as a control landmark to account for any larval movement. Duty Cycle was determined by dividing the number of frames mitochondria moved in the anterograde direction, retrograde direction or paused by the total number of frames and expressed as a percent of total tracking time. Flux was measured in nerve segments by drawing a line down the middle of the bleached area and counting the number of mitochondria that crossed the line in both anterograde and retrograde directions. Mitochondria moving in anterograde and retrograde directions were counted separately, and flux was expressed as the number of moving mitochondria per nerve (n = 21–22 nerve segments). Mitochondrial length was determined by direct measurements using Image J software (NIH, Bethesda, MD) (n = 45–50 mitochondria). The extent of mitochondrial pausing was determined by dividing the total time spent pausing by the number of pauses. For velocity, duty cycle and pauses, 326–360 mitochondria were measured per condition.

2.9. Data analysis and statistics

Data was analyzed and graphs generated using Prism Software (Graph Pad, La Jolla, CA). Statistical analysis was done using One Way ANOVA and Bonferroni's multiple comparisons test.

3. Results

3.1. Cisplatin treatment induces behavior deficiencies without affecting larval survival

To establish the effects of cisplatin on *Drosophila* larvae in vivo we examined the dose response of drug treatment on survival in third instar larvae. Cisplatin did not kill the larvae at 0, 5 and 10 $\mu\text{g/ml}$. However, when the concentration was increased to 25 and 50 $\mu\text{g/ml}$, survival of pupae decreased to 62% and 36% (Fig. 2A). The number of cisplatin-treated larvae that became pupa and subsequently the number of pupa that hatched to adults was counted and expressed as a percent survival of the initial number of larvae added to the assay. Survival of adults was also the same between 0, 5 or 10 $\mu\text{g/ml}$ cisplatin and decreased to 26% and 2% with 25 and 50 $\mu\text{g/ml}$ cisplatin respectively. Cisplatin did not induce a significant decrease in pupa survival with 25 $\mu\text{g/ml}$ but did induce a significant decrease of 53% in adult survival ($p < 0.0001$). Increasing the concentration to 50 $\mu\text{g/ml}$ cisplatin induced a significant decrease of 50% in larvae and 77% in adult survival ($p < 0.0001$).

Our studies then looked at righting, crawling and heat sensing behavior to determine if we could see behavior changes at concentrations that do not kill the larvae. Righting behavior was observed in wandering third instar larvae treated with 0, 10 and 25 $\mu\text{g/ml}$ cisplatin (Fig. 2B). Righting deficiencies were observed in D42-MitoGFP larvae treated with 10 and 25 $\mu\text{g/ml}$ cisplatin. Untreated larvae were able to right themselves in 7.06 s. Cisplatin increased the righting time to 11.98 s with 10 $\mu\text{g/ml}$ cisplatin and 17.28 s with 25 $\mu\text{g/ml}$ cisplatin ($p < 0.0001$). Larvae were then tested for crawling behavior (Fig. 2C) by counting the number of squares the larvae crawled into per minute.

D42-MitoGFP larvae treated with cisplatin were able to crawl into 6.23 squares at 10 $\mu\text{g/ml}$ and 5.79 squares at 25 $\mu\text{g/ml}$. Untreated larvae were able to crawl into 7.03 squares. We found no significant difference between 10 $\mu\text{g/ml}$ cisplatin treated larvae and untreated larvae. However, there was a significant difference between untreated and 25 $\mu\text{g/ml}$ cisplatin treated larvae ($p < 0.01$). To determine if the behavior changes we observed had a sensory component, we tested the larvae for heat sensing behavior (Fig. 2D). Larvae undergo a series of responses to heat exposure as the temperature increases (Chattopadhyay et al., 2012). The initial response is a sensing of the heat with a thrashing of the head back and forth. The larva then undergoes an escape response by rolling and whipping (bringing the head and tail together to make a “C”). This is followed by seizure and paralysis of the larva. Our studies used the head thrash as our behavior response because it is when they first sense heat and relies less on motor coordination. D42-MitoGFP larvae treated with cisplatin became more sensitive to heat. Head thrash was observed at 14.82 s in untreated larvae and cisplatin treatment significantly decreased head thrash time to 10.79 s at 10 $\mu\text{g/ml}$ ($p < 0.001$) and 9.27 s at 25 $\mu\text{g/ml}$ cisplatin ($p < 0.0001$).

3.2. Behavior deficits are inhibited by p35

Cisplatin induces DNA damage, which leads to activation of caspases and neuronal apoptosis (McDonald et al., 2005; McDonald and Windebank, 2002). To determine if caspases were involved in cisplatin-induced behavior deficits, studies were conducted in larvae that expressed p35 in motor neurons. p35 is a pan caspase inhibitor found in baculovirus (Clem, 2007) and can be expressed in *Drosophila* using the GAL4-UAS system (Duffy, 2002).

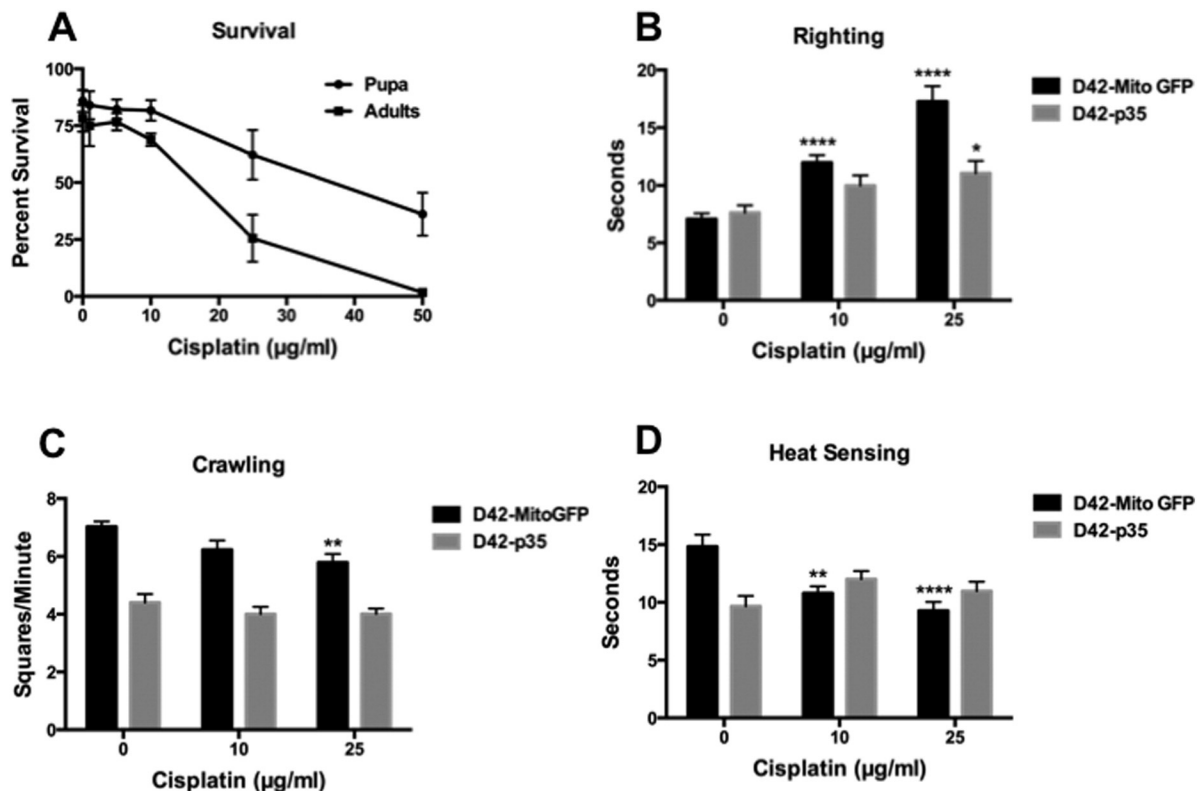


Fig. 2. Cisplatin induces behavior deficiencies at 10 $\mu\text{g/ml}$ without affecting larval survival and behavior deficiencies are inhibited by p35. (A) Survival of cisplatin treated *Drosophila* larvae to pupa and adults developmental stages was determined as a percent of the number of larvae added at the beginning of the experiments. The number of larvae that became pupa and the number of pupa that hatched into adults were calculated as percent survival ($n = 100$ –180 larvae). Larvae treated with 0, 10 and 25 $\mu\text{g/ml}$ cisplatin were observed for righting, crawling and heat sensing abilities. There were significant delays in righting time (B) ($p < 0.0001$), decreases in crawling distance (C) ($p < 0.01$) and increases in heat sensing time (D) ($p < 0.01$ – 0.0001) with 10 and 25 $\mu\text{g/ml}$ cisplatin ($n = 14$ –60 for righting, 30–35 for crawling and 20–27 for heat sensing behavior). Expression of p35 in motor neurons improved righting (B), crawling (C) and heat sensing (D) behavior with no significant differences between untreated and cisplatin treated p35 larvae. However, righting behavior in 25 $\mu\text{g/ml}$ cisplatin treated p35 larvae was significant from untreated p35 larvae ($p < 0.05$) ($n = 14$ –15 larvae) (means and SEM are shown for each data point).

Our studies showed that p35 expression prevented the cisplatin induced behavior changes. No significant difference was observed in righting behavior between untreated and 10 $\mu\text{g/ml}$ cisplatin treated larvae (Fig. 2B). However, there was still a significant difference, though greatly reduced, between untreated and 25 $\mu\text{g/ml}$ cisplatin treated larvae ($p < 0.05$). Righting behavior was 7.61 s in untreated larvae, 9.99 s in larvae treated with 10 $\mu\text{g/ml}$ cisplatin and 11.06 s in larvae treated with 25 $\mu\text{g/ml}$ cisplatin. p35 expression also showed no significant difference in crawling behavior (Fig. 2C). Untreated larvae crawled 4.40 squares compared to 4.00 squares with 10 $\mu\text{g/ml}$ and 4.01 squares with 25 $\mu\text{g/ml}$ cisplatin treated larvae. Heat sensing was also not significantly different between untreated and larvae treated with 10 and 25 $\mu\text{g/ml}$ cisplatin (Fig. 2D). Heat response was observed at 9.66 s in untreated larvae, 12.00 s with 10 $\mu\text{g/ml}$ cisplatin or 10.98 s with 25 $\mu\text{g/ml}$ cisplatin.

3.3. Behavior deficiencies were independent of caspase 3 activation

To determine if cisplatin-induced behavior changes involved active caspase 3, we performed immunohistochemistry in dissected larvae (Fig. 3). Motor neurons (green) from larvae treated with 0 (Fig. 3A), 10 (Fig. 3B) and 25 $\mu\text{g/ml}$ (Fig. 3C) cisplatin were stained for active caspase 3 (red). We found no active caspase 3 staining with 0 $\mu\text{g/ml}$ (Fig. 3D) or 10 $\mu\text{g/ml}$ cisplatin (Fig. 3E). When the concentration was increased to 25 $\mu\text{g/ml}$, active caspase 3 was observed (Fig. 3F). Composite images of GFP motor neurons and active caspase 3 staining (Fig. 3G,H, and I) showed the active caspase 3 induced by 25 $\mu\text{g/ml}$ is co-localized with the mitochondria.

In panel F, we see some red active caspase 3 staining not associated with green mitochondria. The ventral nerve cord contains glial cells and neuroblasts (neural stem cells) (Homem and Knoblich, 2012) and outlying red staining may be due to cisplatin-induced apoptosis in these cells.

3.4. Cisplatin treatment decreases membrane potential and increases reactive oxygen species

To determine the effect of cisplatin on mitochondrial function we first evaluated its effect on mitochondrial membrane potential (MMP) using a specific dye, tetramethylrhodamine methyl ester (TMRM), and confocal fluorescence microscopy. TMRM is readily taken up by actively respiring organelles while mitochondrial membrane depolarization reduces or prevents TMRM uptake. Particle analysis revealed that mitochondrial density was not different in nerves of untreated larvae compared to larvae treated with 10 $\mu\text{g/ml}$ cisplatin (Data not shown). We next compared the co-localization of GFP (green) and TMRM (red) in treated and untreated larvae (Fig. 4A–F). We have found that while most of mitochondria co-localized with TMRM in untreated larvae (Fig. 4E), there were multiple organelles that did not uptake TMRM in larvae treated with 10 $\mu\text{g/ml}$ cisplatin (Fig. 4F, white arrows). Specifically, in larvae treated with 0 $\mu\text{g/ml}$ cisplatin 87% of mitochondria showed red fluorescence indicating the uptake of TMRM. This number was reduced to 60% in 10 $\mu\text{g/ml}$ cisplatin treated animals (Fig. 4H). Increasing the concentration of cisplatin to 25 $\mu\text{g/ml}$ did not further decrease the number of TMRM-positive mitochondria with 62% TMRM uptake. Thus, our data suggest that cisplatin treatment affects mitochondrial membrane potential.

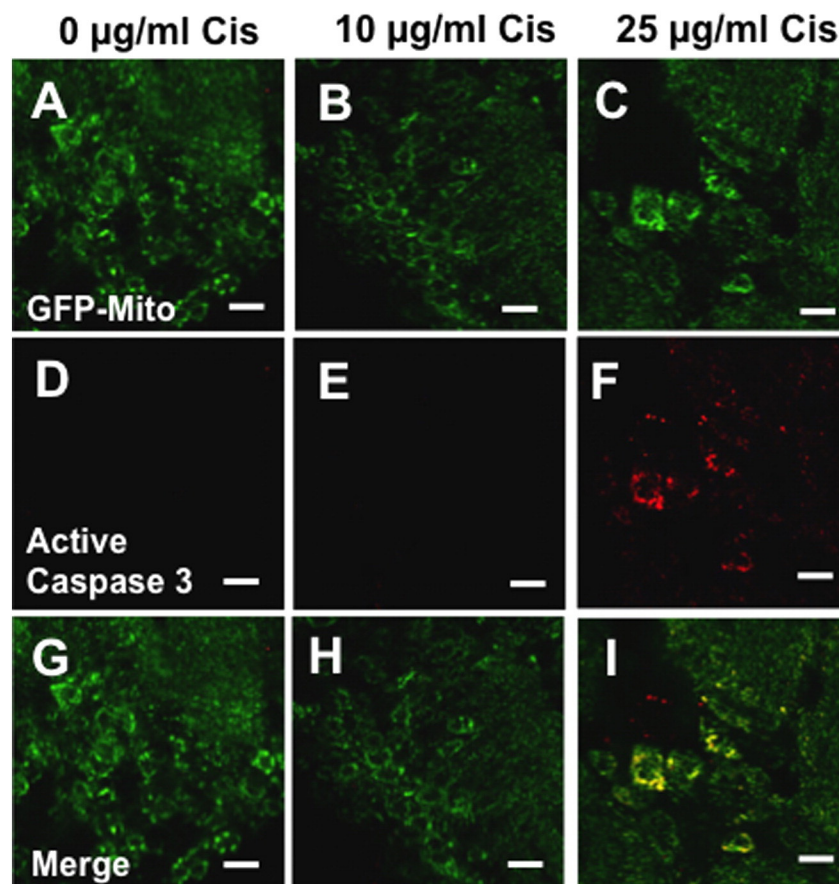


Fig. 3. No active caspase 3 was observed in motor neurons treated with 10 $\mu\text{g/ml}$ cisplatin. Mito-GFP larvae treated with 0, 10 and 25 $\mu\text{g/ml}$ cisplatin were dissected and immunostained for active caspase 3. Images of ventral nerve cord showed no positive staining in Mito-GFP larvae treated with 0 (A, D, G) and 10 (B, E, H) $\mu\text{g/ml}$ cisplatin. Increasing cisplatin concentration to 25 $\mu\text{g/ml}$ induced active caspase 3 (C, F) in mitochondria (I). Images were acquired using a LSM 780 Axio Observer microscope with a 40 \times lens (C-apochromat/1.20 W). Scale bar 2.5 μm .

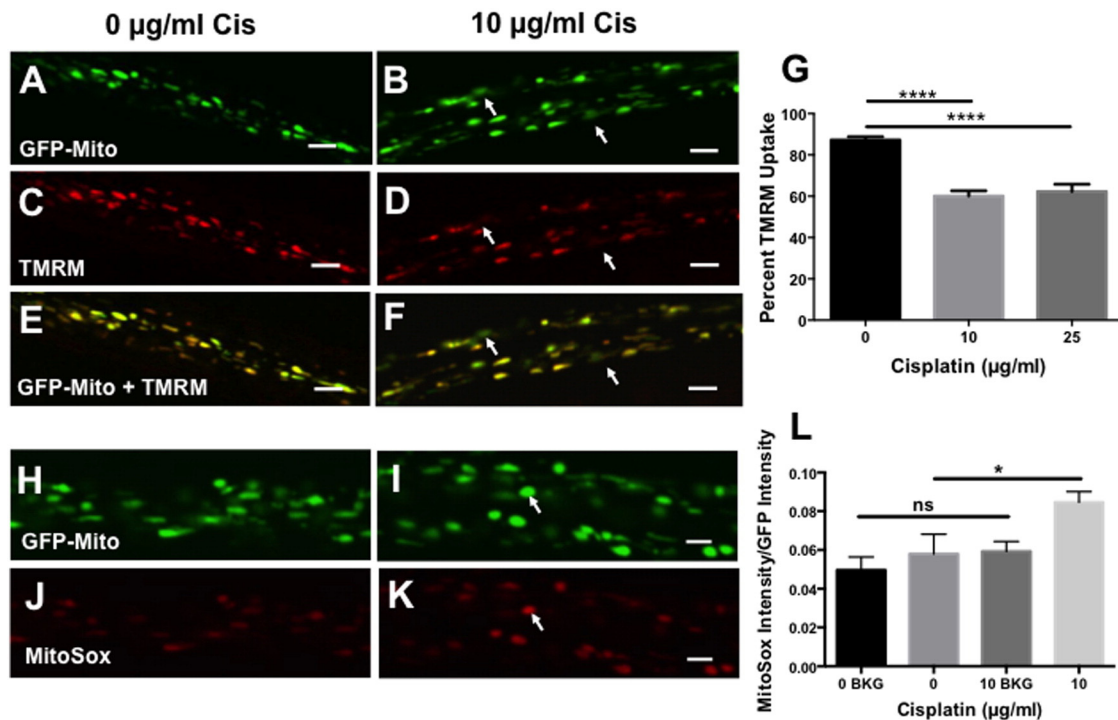


Fig. 4. Cisplatin induces a decrease in mitochondrial TMRM uptake and an increase in ROS production. Mito-GFP *Drosophila* larvae treated with 0 (A) and 10 μg/ml (B) cisplatin were stained with 1 μM TMRM (C, D, red). (E, F) Co-localization of green (mitochondrial GFP) and red (TMRM uptake) fluorescence in larval segmental nerve. (G) Percent of GFP-tagged mitochondria that uptake TMRM. Analysis was done in 34–79 nerve segments from 17 to 38 larvae ($p < 0.0001$). Scale bar 30 μm. Mito-GFP *Drosophila* larvae treated with 0 (H) and 10 μg/ml cisplatin (I) and stained for ROS using 5 nM MitoSox (J, K, red). (L) Cisplatin significantly increased mitochondrial ROS as indicated by the oxygen radical sensor, MitoSox. Analysis was done in 26–41 nerve segments from 7 to 16 larvae ($p < 0.05$). Scale bar 300 μm. Images were acquired using an Olympus Multiphoton Laser Scanning microscope with a 60× lens (UPLSAPO/1.2 W). (Means and SEM are shown for each data point.)

To determine the consequences of mitochondrial membrane depolarization induced by cisplatin, we examined levels of reactive oxygen species (ROS) production using the oxygen radical sensitive dye MitoSox (Onizuka et al., 2011). MitoSox is readily oxidized by superoxide inducing red fluorescence, which can be quantitated using fluorescence microscopy. ROS was tested in 0 and 10 μg/ml cisplatin only because 25 μg/ml did not result in a higher TMRM uptake deficiency. When MitoSox red fluorescence (Fig. 5J, and K) was normalized against Mito green fluorescence (Fig. 5H, and I), we found a significant increase in mitochondrial ROS in larvae treated with 10 μg/ml cisplatin compared to untreated animals (Fig. 4L) ($p < 0.05$).

3.5. Cisplatin treatment does not affect mitochondrial axonal motility, flux or length of the organelles

Changes in mitochondrial membrane potential can affect mitochondrial axonal trafficking (Miller and Sheetz, 2004). We therefore examined the effects of cisplatin treatment on mitochondrial dynamics using live imaging. Larvae treated with 0 and 10 μg/ml cisplatin were observed for segmental nerve mitochondrial movement. Mitochondrial trafficking in motor neurons (Fig. 5A) was observed using confocal microscopy, which allowed estimation of mitochondrial velocity in anterograde and retrograde directions, organelle flux, and length of the organelles in larvae treated with 0 or 10 μg/ml cisplatin. In untreated larvae and in larvae treated with 10 μg/ml cisplatin, the average velocity of mitochondria moving in the anterograde direction was the same 0.35 μm/s. Retrograde mitochondria moved at a velocity of 0.43 μm/s in untreated larvae and at 0.41 μm/s in larvae treated with 10 μg/ml cisplatin. Cisplatin did not alter the number of moving mitochondria (flux) in either the anterograde or retrograde direction (Fig. 5C). Thus, on average 20.14 mitochondria were moving in anterograde direction in untreated larvae compared to 15.67 in larvae treated with 10 μg/ml

cisplatin. The number of mitochondria moving in the retrograde direction was 14.23 in untreated compared to 12.24 in larvae treated with 10 μg/ml cisplatin. Mitochondrial length was also unchanged by cisplatin treatment (Fig. 5D). The average length of mitochondria moving in the anterograde direction in untreated larvae was 1.39 μm compared to 1.36 μm in larvae treated with 10 μg/ml cisplatin. The average length of mitochondria moving in the retrograde direction was 1.25 μm and 1.24 μm in untreated and treated larvae respectively.

3.6. Cisplatin increases time mitochondria spent pausing

Mitochondria are dynamic organelles that undergo bi-directional movement along the axons. It is also well established that along with the smooth movement, mitochondria often switch the direction and tend to pause (Trushina et al., 2004). The pattern of mitochondrial motility and time they spend in motion versus stationary state could indicate abnormalities associated with the function of motor proteins, changes in ATP and calcium levels or stability of cytoskeleton and microtubule tracks (Chang et al., 2011; Lin and Sheng, 2015; Niescier et al., 2013). Since we did not detect any differences in mitochondrial velocities and flux in cisplatin treated larvae, we next examined the amount of time mitochondria spent in a moving vs. stationary state (Fig. 6A).

Using live imaging we found that cisplatin treatment significantly reduced the amount of time mitochondria spent moving in the retrograde direction. Specifically, the amount of time mitochondria moved in the anterograde direction, retrograde direction or paused was calculated as a percent of the total time measured. Cisplatin did not alter anterograde movement of the organelles but significantly decreased retrograde movements ($p < 0.05$) and significantly increased the amount of time paused ($p < 0.01$). (Fig. 6A) Kymographs of mitochondrial movement generated using real-time imaging in untreated vs.

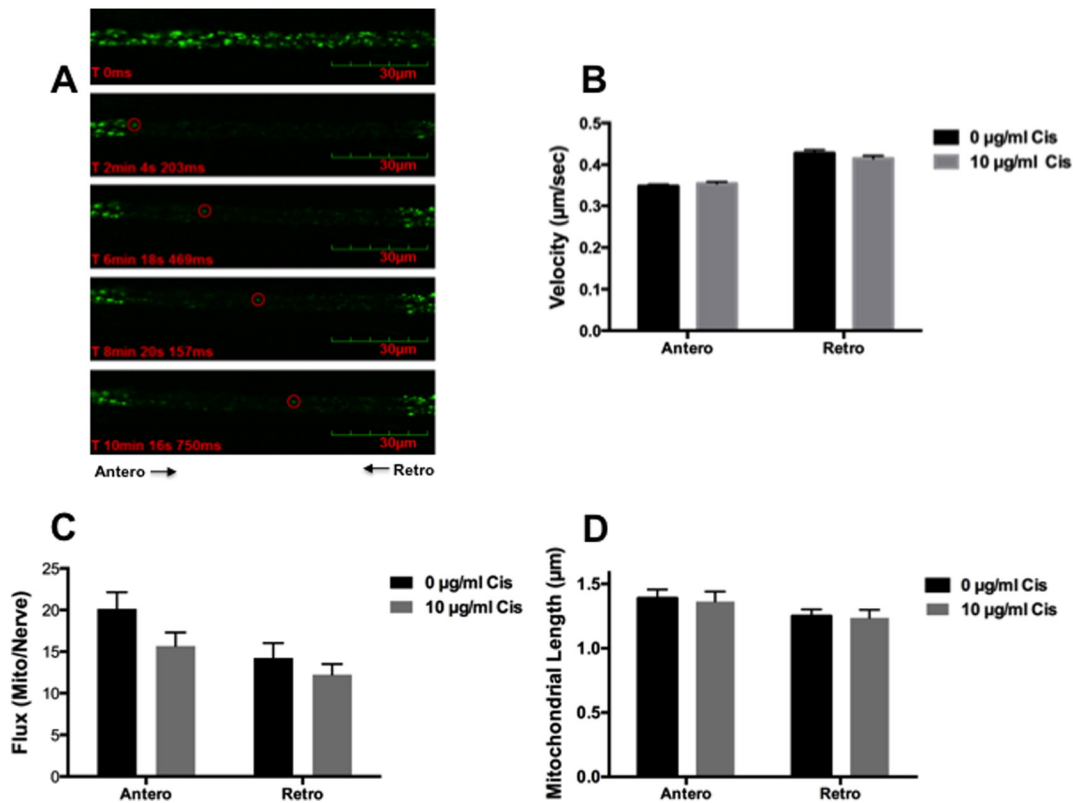


Fig. 5. Treatment with cisplatin does not affect the velocity of mitochondrial motility in axons, the number of moving organelles or their length. (A) Real time imaging of mitochondrial movement within the motor neurons of live third instar larvae recorded using confocal fluorescence microscopy. All mitochondria express GFP (top image). Central area of the nerve was photo bleached (second image from the top) to visualize mitochondrial movement. The progression of the circled organelle along the axon could be seen in the consecutive images. Scale bar, 30 μm . Images were acquired using an Olympus Multiphoton Laser Scanning microscope (FV1000MPE) with a 60 \times lens (UPLSAPO/1.2 W). (B) Velocity of mitochondria was determined by dividing the total distance (μm) traveled by the total time spent in motion (s). A total of 326–360 mitochondria were measured per condition for velocity. (C) Mitochondrial flux measured the number of mitochondria moving across the axon in the anterograde and retrograde direction. Flux was measured in 21–22 nerve segments from 16 to 17 larvae. (D) Mitochondrial length was measured in 45–50 larvae (μm). (Means and SEM are shown for each data point.)

treated larvae allow to evaluate motile organelles compared to stationary organelles based on their net direction of motion (Fig. 6B–E). Cisplatin treatment increased the amount of time mitochondria spent pausing irrelevant of the direction of the net movement (Fig. 6D and E; white bars).

The kymographs indicate that the length of mitochondrial pauses was longer for mitochondria moving in the net retrograde direction compared to mitochondria moving in the net anterograde direction. Therefore we next quantitated the percent of total time mitochondria spent pausing (Fig. 6F) and the length of pauses separately (Fig. 6G). Pausing was significantly increased in both mitochondria moving in the net anterograde ($p < 0.01$) and net retrograde direction ($p < 0.001$). We found no significant difference in pause length for mitochondria moving in the net anterograde direction between treated and untreated animals. However, a significant difference was observed in mitochondria moving in the net retrograde direction with an average pause of 1.78 s in untreated and 2.24 s in cisplatin treated larvae ($p < 0.05$).

4. Discussion

Cellular mechanisms underlying CIPN are not well understood. Emerging evidence suggests that disruption of mitochondrial dynamics and function including axonal transport could underlie and contribute to CIPN (Katsetos et al., 2013). This is consistent with the observations that CIPN mainly affects sensory neurons with the long processes supporting the hypothesis that altered delivery of mitochondria to the distal sites of the axons could induce axonal degeneration leading to neuronal dysfunction and symptoms of neuropathy (Carozzi et al.,

2015; Chan, 2006; Sheng and Cai, 2012). Cisplatin, taxol and bortezomib are chemotherapeutic agents with different cellular targets that affect mitochondria function and induce peripheral neuropathy. Taxol binds directly to microtubules and Bortezomib induces tubulin polymerization (Carozzi et al., 2015; Staff et al., 2013). Both agents affect microtubules dynamics and interrupt axonal trafficking of vesicles and organelles including mitochondria. Cisplatin binds DNA, inducing DNA damage and apoptosis (McDonald et al., 2005; McDonald and Windebank, 2002). Formation of Pt-mtDNA adducts inhibits mtDNA replication and transcription but the role mitochondria play in peripheral neuropathy is not well understood (Podratz et al., 2011a). One of the obstacles in revealing the molecular mechanisms of CIPN is the lack of a robust model to monitor the effect of chemotherapy drugs on mitochondrial axonal trafficking and function.

We have previously utilized an adult *Drosophila* model to demonstrate that cisplatin induced a neuron specific climbing deficiency associated with neuronal apoptosis in the brain (Podratz et al., 2011b). Adult *Drosophila* fed cisplatin for three days had normal survival with deficiencies in geotaxis climbing behavior. In climbing deficient flies, brain neurons stained positive for active caspase 3. Both active caspase 3 and climbing deficiencies were prevented by expression of a pan caspase inhibitor, p35, specifically in brain neurons. In mammals, cisplatin does not cross the blood brain barrier and affects predominantly sensory neurons (Gregg et al., 1992; Thompson et al., 1984). However, the *Drosophila* blood brain barrier consists of only two glial cell types and does not exclude cisplatin (Podratz et al., 2011b; Schirmeier et al., 2015). This allows for study of various neurons in the fly. In the present work we utilized *Drosophila* larvae to monitor the effect of cisplatin on mitochondrial axonal motility and function in intact nervous system

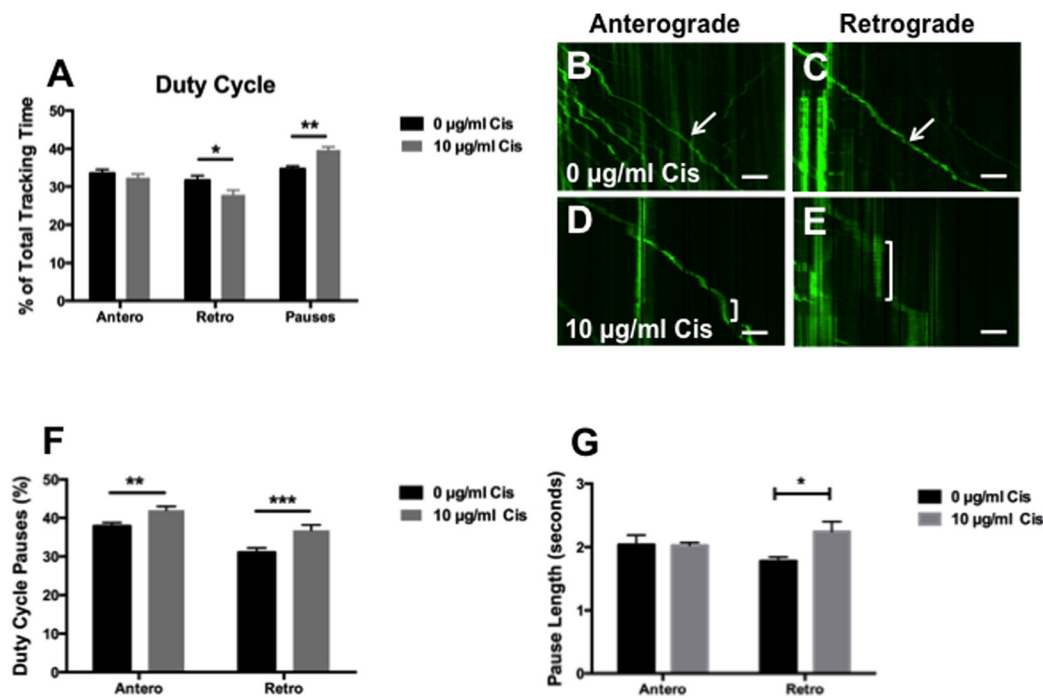


Fig. 6. Cisplatin increased the number and length of mitochondrial pausing along the axon. (A) Mitochondria were quantitated for the percent of total time spend moving in the anterograde and retrograde direction or paused. Duty cycle was measured in 328–360 mitochondria ($p < 0.05$ – $p < 0.01$). Kymographs of mitochondria in untreated (B, C) and treated (D, E) motor neurons show overall movement with time (X axis) verse distance (Y axis). White arrows in (B) and (C) represent organelles moving in the net anterograde and retrograde directions, respectively. Images were acquired using an Olympus Multiphoton Laser Scanning microscope (FV1000MPE) with a 60 \times lens (UPLSAPO/1.2 W). Scale bar 30 μ m. Larvae treated with 10 μ g/ml cisplatin showed longer pauses (white brackets) in both the (D) anterograde and (E) retrograde net direction. (F) Pauses separated into net anterograde or net retrograde moving mitochondria show increased pausing in both directions. (G) The length of pauses of mitochondria moving in the anterograde and retrograde net direction. (F) Pauses separated into net anterograde or net retrograde moving mitochondria show increased pausing in both directions. (G) The length of pauses of mitochondria moving in the anterograde and retrograde net direction. (Means and SEM are shown for each data point.)

in real time. Segmental nerve is easy to visualize and drug effects on proximal or distal nerve can be separated. The additional advantage of this model is the ability to precisely identify GFP-expressing mitochondria. Moreover, axonal trafficking machinery is highly conserved between *Drosophila* and mammals making fly a good model for mechanistic studies (Lloyd, 2012).

Our data suggests that mitochondrial deficiencies occur early in cisplatin-induced neurotoxicity. Both nDNA and mtDNA form adducts with cisplatin at a similar rate and adducts are repaired by nucleotide excision repair (NER) in the nucleus. Because mitochondria do not have the machinery for NER, we would expect Pt-mtDNA adducts to remain in the mitochondria making them more sensitive to cisplatin. We have previously shown that cisplatin binds to mtDNA in primary DRG neurons inhibiting mtDNA replication and transcription, in vitro (Podratz et al., 2011a). MtDNA provide necessary proteins for the different protein complexes within the electron transport chain (ETC) and interruption of the ETC could contribute to the increased ROS production and mitochondrial membrane depolarization. In this study we confirmed that cisplatin induced mitochondrial membrane depolarization, increased production of ROS and altered mitochondrial dynamics in larvae segmental nerves at a non-lethal concentration of cisplatin. These mitochondrial changes were found in righting and heat sensing deficient third instar larvae (Fig. 7) and involved both motor and sensory signalling. These results support the hypothesis that mitochondria are primary and early targets in cisplatin-induced neurotoxicity.

Expression of p35 in motor neurons prevented the cisplatin-induced behavior changes in our study. However, we were not able to visualize active caspase 3 at 10 μ g/ml cisplatin. p35 is an established inhibitor of caspase activity, preventing apoptosis in *Drosophila* (Clem, 2007). It has also been reported to induce cell transformation (Resnicoff et al., 1998) transcription upregulation (Takramah et al., 2003) and translation inhibition (Thiem and Chejanovsky, 2004). It has been recently shown that p35 is involved in the baculovirus defense system against

host antiviral response by inhibiting RNAi (Gammon and Mello, 2015;

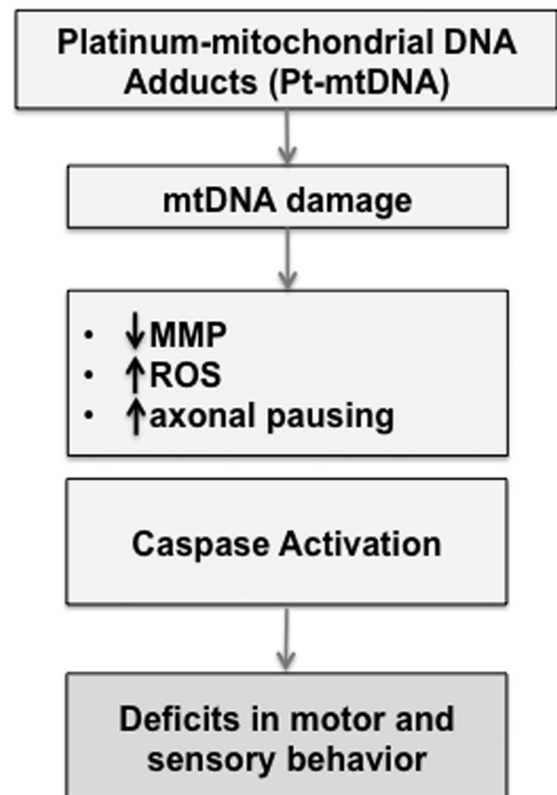


Fig. 7. Model of cisplatin-induced neurotoxicity.

Mehrabadi et al., 2015). Mehrabadi found p35 RNAi interference was independent of its anti-apoptotic effects. It is possible that p35 protection against behavior deficits may involve an apoptosis independent mechanism. It is also possible the levels of active caspase 3 were below detection levels using immunohistochemistry. We observed mitochondrial deficits in the axon at 10 $\mu\text{g}/\text{ml}$ cisplatin, which did lead to detectable active caspase 3 when we increased the concentration to 25 $\mu\text{g}/\text{ml}$. In mammalian neurons, active caspase 3 is observed in the axon of degenerating neurons (King et al., 2013; Simon et al., 2012; Sokolowski et al., 2014). It is possible that localized caspase 3 activation may occur in the axon. If active caspase 3 is involved in the behavior changes observed at 10 $\mu\text{g}/\text{ml}$ cisplatin, the occurrence of apoptosis would be very low.

Significant changes in mitochondrial membrane potential and increased levels of ROS did not lead to significant changes in mitochondrial axonal trafficking deficiencies. In our study, mitochondrial velocity, duty cycle, flux and length were measured in the motile mitochondria while TMRM uptake and ROS were measured in all mitochondria. Motile mitochondria comprise about 20–30% of total mitochondria with the remainder anchored to neurofilaments along the axon (Lin and Sheng, 2015). Stationary mitochondria provide most of the ATP for axonal processes and regulate calcium levels. Mitochondrial calcium may regulate local calcium levels along the axon and dissociates motor proteins from the microtubule inducing motile mitochondria to stop (Lin and Sheng, 2015). Uncoupled mitochondria can also lead to mitochondrial dysfunction, decreased axonal ATP, mitochondrial fission/fusion and mitophagy of damaged mitochondria (Lemasters, 2014; Lin and Sheng, 2015). The decreased TMRM uptake and increased ROS observed in this study indicate that some mitochondria are uncoupled. However, the lack of changes in velocity, flux and mitochondrial size indicates that mitochondrial uncoupling was most likely transient. It is possible that cisplatin induces transient deficiencies in the mitochondria, which lead to localized calcium release. The resulting increase in calcium levels could cause the motile mitochondria to stop until the healthy mitochondria buffer calcium levels to normal. It is possible that interruption of mitochondrial trafficking and intermittent mitochondrial deficiencies are key factors in cisplatin-induced neurotoxicity.

In patients, cisplatin-induced peripheral neuropathy is associated with cumulative doses beginning at 250–350 mg/m^2 (Grisold et al., 2012). Often symptoms occur later in treatment after multiple cycles of chemotherapy and can continue for months after treatment is stopped. In our experiments, the *Drosophila* larvae received a single three-day treatment, which decreased the number of active mitochondrial. Patients receive multiple treatment cycles interspersed with periods of rest. It is possible that mitochondrial homeostasis is affected with the first cycle of treatment in patients, which exacerbates mitochondrial sensitivity in successive cycles. Specific targeting of mitochondria by cisplatin has been found to be effective in killing cisplatin-resistant cancer cells (Marrache et al., 2014; Suntharalingam et al., 2014). Mitochondria-targeted antioxidants have also been successful in preventing cisplatin-induced mitochondrial dysfunction and toxicity in renal cells (Mukhopadhyay et al., 2012). These studies indicate that mitochondria can determine the fate of cisplatin treated cells. This may be particularly true for neurons due to their unique dependency on mitochondrial respiration. Early interventions protecting mitochondria may help prevent neurotoxicity, allowing higher doses of the drug to be used for better cancer treatment.

5. Conclusions

Our studies showed that cisplatin induces deficiencies in righting and heat sensing behavior in *Drosophila* larvae without killing animals. Behavior changes were abrogated by p35 but apparently independent of active caspase 3. In behavior deficient larvae, cisplatin decreased the number of active mitochondria and increased the amount of mitochondrial pausing during axonal trafficking. These results indicate that

mitochondrial function is affected before the neuron is committed to undergo apoptosis and suggest that it is the mitochondrial dysfunction that is responsible for neurotoxicity.

Supplementary data to this article can be found online at <http://dx.doi.org/10.1016/j.nbd.2016.10.003>.

Acknowledgments

This study was supported by the Mayo Clinic Center for Regenerative Medicine, Mayo Graduate School and CTSA Grant numbers TL1 TR000137 and UL1 TR000135 from the National Center for Advancing Translational Science (NCATS). Its contents are solely the responsibility of the authors and do not necessarily represent the official views of the NIH. We thank Jane Meyer for her administrative role in manuscript preparation.

References

- Albers, J.W., et al., 2011. Interventions for preventing neuropathy caused by cisplatin and related compounds. *Cochrane Database Syst. Rev.* CD005228.
- Carozzi, V.A., et al., 2015. Chemotherapy-induced peripheral neuropathy: what do we know about mechanisms? *Neurosci. Lett.* 596, 90–107.
- Cavaletti, G., Marmiroli, P., 2010. Chemotherapy-induced peripheral neurotoxicity. *Nat. Rev. Neurol.* 6, 657–666.
- Chan, D.C., 2006. Mitochondria: dynamic organelles in disease, aging, and development. *Cell* 125, 1241–1252.
- Chang, K.T., et al., 2011. Mitochondrial matrix Ca^{2+} as an intrinsic signal regulating mitochondrial motility in axons. *U.S.A. J. Proc. Natl. Acad. Sci. U.S.A.* 108, 15456–15461.
- Chattopadhyay, A., et al., 2012. Local and global methods of assessing thermal nociception in *Drosophila* larvae. *J. Vis. Exp.*, e3837.
- Clem, R.J., 2007. Baculoviruses and apoptosis: a diversity of genes and responses. *Curr. Drug Targets* 8, 1069–1074.
- Croteau, D.L., et al., 1999. Mitochondrial DNA repair pathways. *Mutat. Res.* 434, 137–148.
- Duffy, J.B., 2002. GAL4 system in *Drosophila*: a fly geneticist's Swiss army knife. *Genesis* 34, 1–15.
- Eastman, A., 1987. The formation, isolation and characterization of DNA adducts produced by anticancer platinum complexes. *Pharmacol. Ther.* 34, 155–166.
- Fischer, S.J., et al., 2001. Alterations in cell cycle regulation underlie cisplatin induced apoptosis of dorsal root ganglion neurons *in vivo*. *Neurobiol. Dis.* 8, 1027–1035.
- Gammon, D.B., Mello, C.C., 2015. RNA interference-mediated antiviral defense in insects. *Curr. Opin. Insect Sci.* 8, 111–120.
- Gill, J.S., Windebank, A.J., 1998. Cisplatin-induced apoptosis in rat dorsal root ganglion neurons is associated with attempted entry into the cell cycle. *J. Clin. Invest.* 101, 2842–2850.
- Gregg, R.W., et al., 1992. Cisplatin neurotoxicity: the relationship between dosage, time, and platinum concentration in neurologic tissues, and morphologic evidence of toxicity. *J. Clin. Oncol.* 10, 795–803.
- Grisold, W., et al., 2012. Peripheral neuropathies from chemotherapeutics and targeted agents: diagnosis, treatment, and prevention. *Neuro-Oncology* 14 (Suppl. 4), iv45–iv54.
- Homem, C.C., Knoblich, J.A., 2012. *Drosophila* neuroblasts: a model for stem cell biology. *Development* 139, 4297–4310.
- Johnson, C., et al., 2015. Candidate pathway-based genetic association study of platinum and platinum-taxane related toxicity in a cohort of primary lung cancer patients. *J. Neurol. Sci.* 349, 124–128.
- Katsetos, C.D., et al., 2013. Mitochondrial dysfunction in neuromuscular disorders. *Semin. Pediatr. Neurol.* 20, 202–215.
- King, A.E., et al., 2013. Excitotoxin-induced caspase-3 activation and microtubule disintegration in axons is inhibited by taxol. *Acta Neuropathol. Commun.* 1, 59.
- Larsen, N.B., et al., 2005. Nuclear and mitochondrial DNA repair: similar pathways? *Mitochondrion* 5, 89–108.
- Lemasters, J.J., 2014. Variants of mitochondrial autophagy: types 1 and 2 mitophagy and micromitophagy (type 3). *Redox Biol.* 2, 749–754.
- Lin, M.Y., Sheng, Z.H., 2015. Regulation of mitochondrial transport in neurons. *Exp. Cell Res.* 334, 35–44.
- Lloyd, T.E., 2012. Axonal transport disruption in peripheral nerve disease: from Jack's discoveries as a resident to recent contributions. *J. Peripher. Nerv. Syst.* 17 (Suppl. 3), 46–51.
- Marrache, S., et al., 2014. Detouring of cisplatin to access mitochondrial genome for overcoming resistance. *U.S.A. J. Proc. Natl. Acad. Sci. U.S.A.* 111, 10444–10449.
- McDonald, E.S., Windebank, A.J., 2002. Cisplatin-induced apoptosis of DRG neurons involves Bax redistribution and cytochrome c release but not fas receptor signaling. *Neurobiol. Dis.* 9, 220–233.
- McDonald, E.S., et al., 2005. Cisplatin preferentially binds to DNA in dorsal root ganglion neurons *in vitro* and *in vivo*: a potential mechanism for neurotoxicity. *Neurobiol. Dis.* 18, 305–313.
- Mehrabadi, M., et al., 2015. The baculovirus antiapoptotic p35 protein functions as an inhibitor of the host RNA interference antiviral response. *J. Virol.* 89, 8182–8192.
- Miller, K.E., Sheetz, M.P., 2004. Axonal mitochondrial transport and potential are correlated. *J. Cell Sci.* 117, 2791–2804.

- Miltenburg, N.C., Boogerd, W., 2014. Chemotherapy-induced neuropathy: a comprehensive survey. *Cancer Treat. Rev.* 40, 872–882.
- Mukhopadhyay, P., et al., 2012. Mitochondrial-targeted antioxidants represent a promising approach for prevention of cisplatin-induced nephropathy. *Free Radic. Biol. Med.* 52, 497–506.
- Niescier, R.F., et al., 2013. Miro, MCU, and calcium: bridging our understanding of mitochondrial movement in axons. *Front. Cell. Neurosci.* 7, 148.
- Onizuka, S., et al., 2011. Lidocaine depolarizes the mitochondrial membrane potential by intracellular alkalization in rat dorsal root ganglion neurons. *J. Anesth.* 25, 229–239.
- O'Reilly, A., et al., 2014. Lhermitte's phenomenon and platinum, beware of latency. *Oncol. Res. Treat.* 37, 591–594.
- Pilling, A.D., et al., 2006. Kinesin-1 and Dynein are the primary motors for fast transport of mitochondria in *Drosophila* motor axons. *Mol. Biol. Cell* 17, 2057–2068.
- Podratz, J.L., et al., 2011a. Cisplatin induced mitochondrial DNA damage in dorsal root ganglion neurons. *Neurobiol. Dis.* 41, 661–668.
- Podratz, J.L., et al., 2011b. *Drosophila melanogaster*: a new model to study cisplatin-induced neurotoxicity. *Neurobiol. Dis.* 43, 330–337.
- Reinstein, L., et al., 1980. Peripheral neuropathy after cis-platinum (II) (DDP) therapy. *Arch. Phys. Med. Rehabil.* 61, 280–282.
- Resnicoff, M., et al., 1998. The baculovirus anti-apoptotic p35 protein promotes transformation of mouse embryo fibroblasts. *J. Biol. Chem.* 273, 10376–10380.
- Savitskaya, M.A., Onishchenko, G.E., 2015. Mechanisms of apoptosis. *Biokhimiya/Biochemistry* 80, 1393–1417.
- Schirmeier, S., et al., 2015. Axon ensheathment and metabolic supply by glial cells in *Drosophila*. *Brain Res.*
- Sheng, Z.H., Cai, Q., 2012. Mitochondrial transport in neurons: impact on synaptic homeostasis and neurodegeneration. *Nat. Rev. Neurosci.* 13, 77–93.
- Shidara, Y., Hollenbeck, P.J., 2010. Defects in mitochondrial axonal transport and membrane potential without increased reactive oxygen species production in a *Drosophila* model of Friedreich ataxia. *J. Neurosci.* 30, 11369–11378.
- Simon, D.J., et al., 2012. A caspase cascade regulating developmental axon degeneration. *J. Neurosci.* 32, 17540–17553.
- Sokolowski, J.D., et al., 2014. Caspase-mediated cleavage of actin and tubulin is a common feature and sensitive marker of axonal degeneration in neural development and injury. *Acta Neuropathol. Commun.* 2, 16.
- Staff, N.P., et al., 2013. Bortezomib alters microtubule polymerization and axonal transport in rat dorsal root ganglion neurons. *Neurotoxicology* 39, 124–131.
- Suntharalingam, K., et al., 2014. A dual-targeting, p53-independent, apoptosis-inducing platinum(II) anticancer complex, [Pt(BDI(QQ))Cl]. *Metallomics* 6, 437–443.
- Ta, L.E., et al., 2006. Neurotoxicity of oxaliplatin and cisplatin for dorsal root ganglion neurons correlates with platinum-DNA binding. *Neurotoxicology* 27, 992–1002.
- Ta, L.E., et al., 2009. Mice with cisplatin and oxaliplatin-induced painful neuropathy develop distinct early responses to thermal stimuli. *Mol. Pain* 5, 9.
- Takramah, D., et al., 2003. Baculovirus P35 interacts with a subunit of human RNA polymerase II and can enhance promoter activity in human cells. *J. Gen. Virol.* 84, 3011–3019.
- Thiem, S.M., Chejanovsky, N., 2004. The role of baculovirus apoptotic suppressors in AcMNPV-mediated translation arrest in Ld652Y cells. *Virology* 319, 292–305.
- Thompson, S.W., et al., 1984. Cisplatin neuropathy. Clinical, electrophysiologic, morphologic, and toxicologic studies. *Cancer* 54, 1269–1275.
- Trushina, E., et al., 2004. Mutant huntingtin impairs axonal trafficking in mammalian neurons in vivo and in vitro. *Mol. Cell. Biol.* 24, 8195–8209.
- Windebank, A.J., Grisold, W., 2008. Chemotherapy-induced neuropathy. *J. Peripher. Nerv. Syst.* 13, 27–46.
- Yeh, E., et al., 1995. Green fluorescent protein as a vital marker and reporter of gene expression in *Drosophila*. *Proc. Natl. Acad. Sci. U. S. A.* 92, 7036–7040.